JMR Journal of Meteorological Research

Springer PIIJ

An Improved Method for Defining Short-Term Climate Anomalies

Xuan CHEN, Tim LI

Citation: , 2021: An Improved Method for Defining Short-Term Climate Anomalies. *J. Meteor. Res.*, **35**(6), 1012-1022, doi: 10.1007/s13351-021-1139-2

View online: http://jmr.cmsjournal.net/article/doi/10.1007/s13351-021-1139-2

An Improved Method for Defining Short-Term Climate Anomalies

Xuan CHEN[1] and Tim LI[1,2*]

1 *Key Laboratory of Meteorological Disaster, Ministry of Education (KLME)/Joint International Research Laboratory of Climate and Environment Change (ILCEC)/Collaborative Innovation Center on Forecast and Evaluation of Meteorological Disasters (CIC-FEMD), Nanjing University of Information Science &Technology, Nanjing* 210044, *China*

2 *International Pacific Research Center and Department of Atmospheric Sciences, School of Ocean and Earth Science and Technology, University of Hawaii at Manoa, Honolulu, HI* 96822, *USA*

(Received July 26, 2021; in final form September 7, 2021)

ABSTRACT

A conventional method to define short-term climate anomalies for atmospheric and oceanic variables, recommended by the World Meteorological Organization (WMO), is the departure from a 30-yr climatological mean in the preceding three decades. Such a method, however, introduces spurious errors such as sudden jumps and artificial trends. A new method, named a trend correctional method, is introduced to eliminate the errors. To demonstrate the capability of this new method, we examine a set of idealized cases first by superposing a "true" interannual or interdecadal signal onto a linear or a nonlinear trend. Comparing to the conventional method, the trend correctional method is able to retain, to a large extent, the "true" anomaly signals. Next, we examined real-time indices. The anomaly time series derived based on the trend correctional method show a better agreement with the observed anomaly series. The root-mean-square error is greatly improved, comparing to that calculated based on the conventional method. Therefore, the results from both the idealized and real cases demonstrate that the new method has a clear advantage to the conventional method in deriving true climate anomalies, in particular under the ongoing global warming circumstance.

Key words: long-term trend, climate anomaly definition, trend correctional method

Citation: Chen, X., and T. Li, 2021: An improved method for defining short-term climate anomalies. *J. Meteor. Res.*, **35**(6), 1012–1022, doi: 10.1007/s13351-021-1139-2.

1. Introduction

Defining short-term climate anomalies such as El Niño/La Niña events is critical for understanding and predicting the climate variability and change. A conventional method that defines such climate anomalies, recommended by the World Meteorological Organization (WMO), is based on the following two steps: 1) computing the monthly climatology based on the preceding three decades (e.g., for "2001 case" using the time average of 1971–2000 and for "2021 case" using the time average of 1991–2020) from original time series; and 2) subtracting the climatology from original time series to obtain climate anomalies. An obvious drawback of the conventional method is that the impact of long-term trends cannot be eliminated. In addition, a jump from one decade to another may introduce spurious periodic signals and a sudden jump. Under the global warming (Lau and Weng, 1999), as temperature rises, the long-term trends may severely impact the conventional method in capturing high-impact climate events such as El Niño/La Niña (Meyers, 1996; Klein et al., 1999; Lau and Nath, 2000; Terray and Dominiak, 2005), tropical North Atlantic (TNA), and Indian Ocean dipole (IOD) modes.

A similar problem rises for computing the Niño indices proposed by Trenberth and Stepaniak (2001). With a calculation of monthly climatology of every 10 years, the long-term trend's impact still exists in the anomaly time series. For linearly increasing trend cases, the anomaly time series would rise locally (for every 10 years) and jump up or down periodically. For nonlinearly increasing trend cases, the anomaly series would jump up or

Supported by the National Natural Science Foundation of China (42088101), NOAA of US (NA18OAR4310298), and National Science Foundation of US (AGS-2006553).

*Corresponding author: timli@hawaii.edu

down irregularly.

From a theoretical perspective, the ENSO-like climate anomaly should be viewed as real-time meteorological/oceanographic phenomena, which means that their values are independent of the reference time window selected. The anomalies calculated by using the conventional method lead to the following problem: the influence of long-term trends, such as an increasing trend (Turkington et al., 2019), will make it difficult to identify cold events, whose intensity and duration will also be weakened. Taking an El Niño/La Niña event (Trenberth, 1997) as an example, the intensity, property, and duration should not depend on the time window through which the mean climatology is defined.

Motivated by the discussion above, in this paper, we intend to develop a new method, so called "trend correctional method." Using this method, one is able to compute "pure" interannual and interdecadal signals from original time series with long-term trends removed. A strategy is developed to test the validation of this method using idealized time series that contains "true" interannual and interdecadal signals. The root-mean-square errors (RMSEs) calculated based on the conventional and trend correctional methods are further compared. Then, a number of real-time indices are further adopted to demonstrate the advantage of the new method. This paper is organized as following. In Section 2, the data and method are introduced. In Sections 3 and 4, we show the results with idealized and real-time series. The conclusions are given in the last section.

2. Data and method

2.1 *Data and indices*

The data used in this study include Niño indices (1870–2020) from the National Center for Atmospheric Research (NCAR) and University Corporation for Atmospheric Research (UCAR), the Global Temperature Index (GTI, 1880–2020) derived from global-mean monthly temperature data from NASA Goddard Institute for Space Studies Surface Temperature Analysis, version 4 (Lenssen et al., 2019), and the sea surface temperature (SST, monthly 1° × 1° SST dataset from 1850 to 2019) reanalysis data (Hirahara et al., 2014) from Japan Meteorological Agency.

Various indices based on SST reanalysis data are used in the current study to validate the current method. They include the Indian Ocean dipole (IOD) west pole index (IODW; averaged over 10°S–10°N, 50°–70°E), IOD east pole index (IODE; averaged over 10°S–0°, 90°–110°E), the Indian Ocean Basin-Wide SST index (IOBW; averaged over 20°S–20°N, 40°–100°E), an area averaged SST index over an Arctic region near Finland (ARC; 60°–75°N, 20°–45°E) where the SST trend (about 0.9 K century^{-1}) during the past century is the largest over the Arctic, and the tropical North Atlantic index (TNA; averaged over 5.5°–23.5°N, 15°–57.5°W).

2.2 *A trend correctional method*

The conventional method to calculate the short-term climate anomaly at a given year is based on a subtraction of a 30-yr climatology in the preceding three decades. It can be written as:

$$\tilde{a}_i = a_i - \bar{a}_i, \tag{1}$$

where $\bar{a}_i$ is the 30-yr monthly climatology. For any year during a decade such as 1981–1990, the 30-yr period is fixed (i.e., 1951–1980). Equation (1) may be rewritten as:

$$\tilde{a}_i = \sum (a_i - a_k)/30, \tag{2}$$

where subscript i is the ith year such as 1985 and the summation is for k for a reference 30-yr period (such as 1951–1980). In order to remove the trend from an original time series, a central difference formula for a 31-yr period (15 yr before and 15 yr after the reference time i) may be used so that the short-term climate anomaly after removing the trend can be written as:

$$\tilde{a}_i = \sum (2a_i - a_{i-k} - a_{i+k})/m, \quad 0 \leqslant k \leqslant 15, \tag{3}$$

where m = 31. Here in order to keep a temporal symmetry, we change sample number from 30 in Eq. (2) to 31 in Eq. (3).

Term $(2a_i - a_{i-k} - a_{i+k})$ in Eq. (3) has the form of the second-order central difference representing the second-order temporal derivative. With this form, the linear trend or the first-order temporal derivative is eliminated. Equation (3) cannot use for the real-time anomaly calculation because future 15-yr data are unavailable. For example, for this year (i = 2021), the data after 2021 are unavailable. Using the Tayler extension method, the second-order difference form may be represented by using preceding 45-yr data points. Thus, Eq. (3) can be rewritten as:

$$\tilde{a}_i = \sum (2a_i - 5a_{i-k} + 4a_{i-2k} - a_{i-3k})/m, \tag{4}$$

where the summation is for k from 0 to 15, and m keeps the same constant (31).

Each summation term at the right-hand side of Eq. (4) for different k may be written as:

$$\begin{cases} 0, & k=0, \\ (2a_i-5a_{i-1}+4a_{i-2}-a_{i-3})/m, & k=1, \\ (2a_i-5a_{i-2}+4a_{i-4}-a_{i-6})/m, & k=2, \\ (2a_i-5a_{i-3}+4a_{i-6}-a_{i-9})/m, & k=3, \\ \cdots & \\ (2a_i-5a_{i-14}+4a_{i-28}-a_{i-42})/m, & k=14, \\ (2a_i-5a_{i-15}+4a_{i-30}-a_{i-45})/m, & k=15. \end{cases} \tag{4a}$$

Rearranging terms at right side of Eq. (4), this equation can be simplified as

$$\tilde{a}_i = \sum(\gamma_k a_{i-k})/m, \quad 0 \leqslant k \leqslant 45, \tag{5}$$

where the summation is for k from 0 to 45, a_{i-k} is the observation of the year $i-k$, and γ_k is a weighting coefficient. Its value is determined based on the summation of all the terms shown in Eq. (4a). Because term a_{i-1} appears only when $k=1$ in Eq. (4a), thus term a_{i-1} weighting coefficient $\gamma_1=-5$. Term a_{i-2}, on the other hand, appears twice in Eq. (4a) when $k=1$ and 2. As a result, $\gamma_2=-1$. Table 1 lists the values of all the weighting coefficients in Eq. (5). Note that $\sum\gamma_k \equiv 0$.

The anomaly calculated based on Eq. (5) is called "trend correctional method." In the subsequent sections, we will demonstrate that this new method has a great advantage to the conventional method in both the idealized and real-time setting.

3. Validation with idealized time series

One way to validate the trend correctional method in comparison to the conventional method is to use a set of idealized time series with specified interannual and interdecadal signals so that we know the "true" anomalies. These idealized time series are superposed onto a long-term trend that is either linear or nonlinear. The specified linear and nonlinear trends are simply adopted from the observed global surface mean temperature during 1915–2020.

A sinusoidal time series is specified as an idealized interannual SST signal that has a constant amplitude of 2°C and a period of about 4.3 yr. Similarly, a sinusoidal time series with a constant amplitude of 0.8°C and a period of 20 yr is specified as an idealized interdecadal SST signal. They have the following formula:

$$s_1(t) = 2\sin(t/25.64\pi - 0.215), \tag{6}$$

$$s_2(t) = 0.8\sin(t/120\pi - 10.073), \tag{7}$$

where t denotes time in unit of month. The variable $t=1$ corresponds to January 1870, $t=13$ corresponds to January 1871, and so on.

In addition, idealized linear and nonlinear long-term trends are specified, derived based on the global surface temperature reanalysis data. The magnitude of the trends is about 2°C $(100\ \text{yr})^{-1}$ (Hansen et al., 2010). The specified linear and nonlinear trends have the following formula:

$$t_1(t) = 25 + 0.0018t, \tag{8}$$

$$t_2(t) = 25 + 1.11\times10^{-6}t^2. \tag{9}$$

We design total six idealized cases for analysis. Case 1 is the simple summation of the idealized interannual time series and the linear trend. Case 2 is the summation of the idealized interannual time series and the nonlinear trend. Cases 3 and 4 are the summation of the idealized interdecadal time series and the linear/nonlinear trend. Case 5 represents the superposition of the interannual and interdecadal time series and the linear trend. Case 6 is the superposition of the interannual and interdecadal time series and the nonlinear trend. Table 2 lists all the six idealized cases.

Figures 1a–c show the idealized interannual time series and the linear trend specified as well as the total time series that combines the two idealized series. Next,

Table 1. Values of γ_k in Eq. (5)

k	0	1	2	3	4	5	6	7	8	9	10	11	12	13	14	15
γ_k	30	−5	−1	−6	−1	−5	−2	−5	−1	−6	−1	−5	−2	−5	−1	−6
k	16	17	18	19	20	21	22	23	24	25	26	27	28	29	30	31
γ_k	4	0	3	0	4	−1	4	0	3	0	4	−1	4	0	3	0
k	32	33	34	35	36	37	38	39	40	41	42	43	44	45		
γ_k	0	−1	0	0	−1	0	0	−1	0	0	−1	0	0	−1		

Table 2. The list of six idealized cases (s_1 and s_2 represent idealized interannual and interdecadal time series, and t_1 and t_2 denote a linear and a nonlinear trend)

	Interannual case		Interdecadal case		Combined case	
	1	2	3	4	5	6
Ideal signal	s_1		s_2		s_1+s_2	
Long-term trend	t_1	t_2	t_1	t_2	t_1	t_2
Total time series	s_1+t_1	s_1+t_2	s_2+t_1	s_2+t_2	$s_1+s_2+t_1$	$s_1+s_2+t_2$

we apply the conventional and trend correctional methods to derive climate anomalies based on the total time series shown in Fig. 1c. The results are shown in Figs. 1d, e. Because the given 1-yr data in the preceding 45 years are needed, the first year plotted in Fig. 1 is 1915, while actual time series starts from 1870.

For comparison with the "true" climate anomaly, both the calculated and specified anomaly time series are plotted in Figs. 1d, e. Note that there is an ascending trend in the blue line in Fig. 1d, and by subtracting the ith anomaly from the $(i-1)$th anomaly, one may find spurious jumps in 1931, 1961, and 1991. This indicates that the time series derived by the conventional method is inconsistent with the "true" anomaly time series represented by the black line. As a consequence, the intensity and duration of cold events are underestimated.

The anomaly time series derived from the trend correctional method (red curve in Fig. 1e) shows a better match with the "true" signal. An interesting difference between the conventional method and the trend correctional method lies in the symmetry of the anomaly with respect to the value of 0. Note that the anomaly series using the conventional method is asymmetric with respect to 0 (Fig. 1d) whereas the anomaly using the trend correctional method is symmetric with respect to 0. With the trend correctional method, the duration of either cold or warm event is same as the "true" signal, but the intensity is slightly larger.

The conventional method bias is magnified when a nonlinear trend is specified. Figure 2 shows that the nonlinear trend has a greater influence on the anomaly series derived from the conventional method. The values of the blue line in Fig. 2d are larger than those of the black line, and there is a rising trend in the anomaly time series, being inconsistent with the "true" interannual signal. Spurious jump points are seen in 1961 and 1991. The intensity and duration of cold episodes decrease as time goes forward. As a result, it becomes more difficult to monitor cold events toward the end of the record. In contrast, such spurious errors are minimized with the trend correctional method (Fig. 2e). The trend correctional method generated anomaly time series is very close to the "true" signal.

Next, we conduct a parallel examination for the specified interdecadal time series. Figures 3a–c show the "true" time series of the interdecadal signal, a linear and

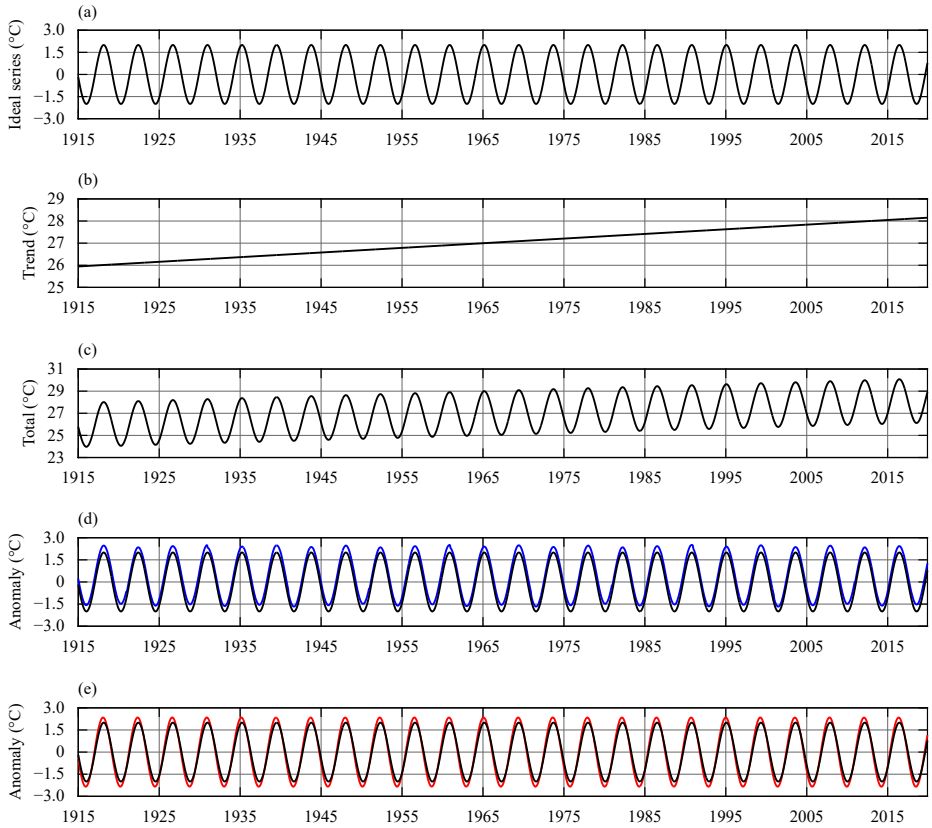

Fig. 1. (a) The specified idealized interannual time series, (b) a linear trend, (c) a sum of (a) and (b) representing a raw time series, (d) an anomaly time series calculated based on the conventional method (blue line), and (e) an anomaly time series derived based on the trend correctional method (red line). The black line in (d, e) denotes the true interannual signal specified. This case denotes Case 1.

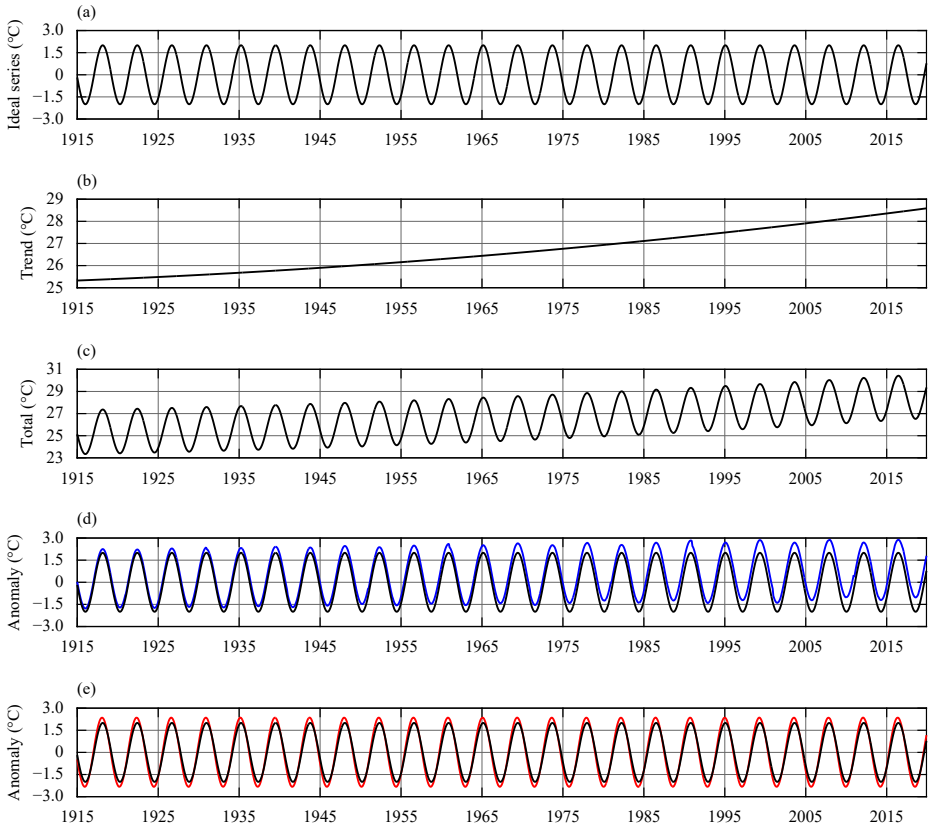

Fig. 2. As in Fig. 1, but for Case 2.

a nonlinear trend, and the total time series. The calculated anomaly time series using the conventional and trend correctional methods are illustrated in Figs. 3d, e. The solid (dashed) lines in the figures represent the results with a nonlinear (linear) trend.

Figure 3 shows that both the linear and nonlinear trends have significant influences on the anomaly series using the conventional method. The values of the blue line in Fig. 3d are greater than those of the black line. Compared to the blue dashed line, there is a significant rising trend in the blue solid line, suggesting that the nonlinear trend has a greater impact. Jump points are seen at the first year of each decade. The cold event intensity and duration are reduced compared to the "true" signals, while the warm event intensity and duration increase. Moreover, the spurious biases are greatly reduced when the trend correctional method is use (Fig. 3e). The calculated anomaly series using the trend correctional method is now symmetric with respect to the normal condition (i.e., the value of 0). The red solid line coincides with the red dashed line, suggesting that the current method is able to handle both the linear and nonlinear trend scenarios.

One may wonder what happens if the conventional method is updated every year instead of every decade. The green curves in Fig. 3d show the result. While the bias becomes smaller compared to the original method, it is still greater than that obtained with the trend correctional method (Fig. 3e), in particular in the nonlinear trend case.

Figure 4 shows the result with the combined interannual and interdecadal signals. The results are in general consistent with those from Figs. 1–3, confirming the usefulness of the current method in deriving the "true" climate signals.

While the temporal correlation coefficients (CC) between the calculated and the specified anomaly series using both the conventional and trend correctional methods are high (greater than 0.95), the advantage of the trend correctional method can be demonstrated clearly by the RMSEs. Figure 5 illustrates that RMSEs using the trend correctional method for all six cases are much less than the ones using the conventional method. This indicates that compared with the conventional method, the trend correctional method has great advantages in both the linear and nonlinear trend cases.

In theory, long-term trends should not affect the calculation of "true" climate anomalies, as natural climate variability does not contain a trend. In the conventional method, the subtraction to the preceding three decadal mean makes arbitrary jumps and spurious trends. For the

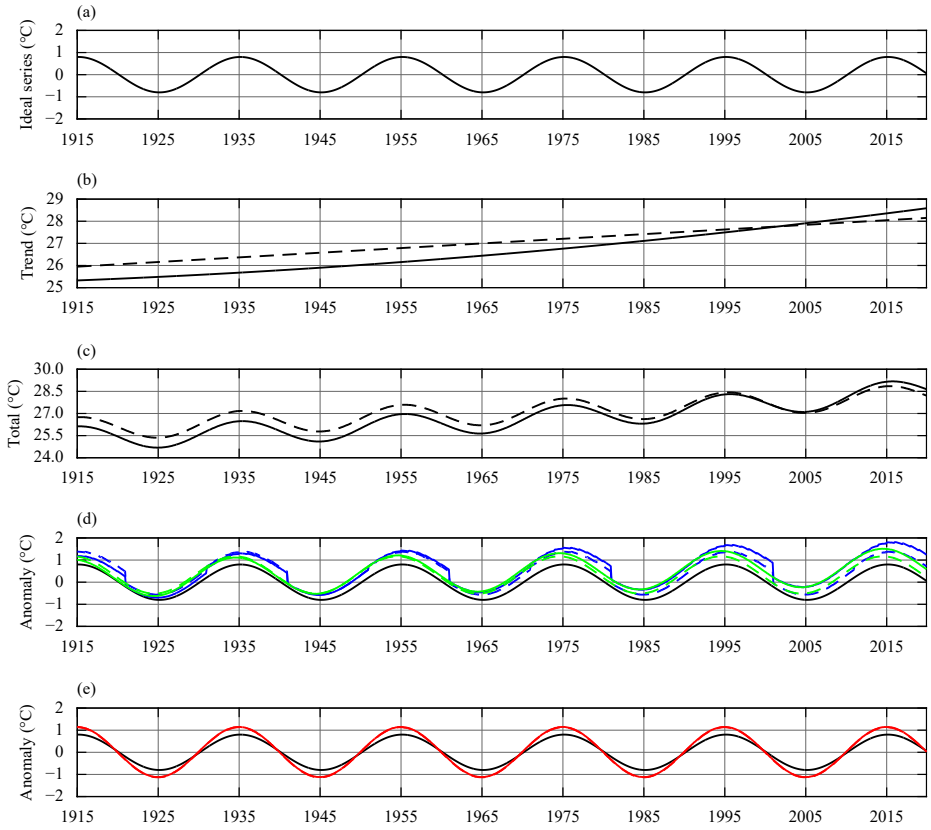

Fig. 3. As in Fig. 1, but for Cases 3 and 4. The black line in (d, e) denotes the true interdecadal signal specified. The green curves in (d) are calculated based on the conventional method but with the climatology being updated every year instead of every decade.

linear trend case just like t_1, an additional spurious period of 10 yr is introduced. During each decade, the anomaly series holds the same trend so that the influence of the linear trend is local. For the nonlinear trend case as t_2, the spurious 10-yr period is also seen. In addition, some longer period bias may also be introduced in the time series, making its impact non-local.

The trend correctional method overcomes the shortcomings of the conventional method. The anomaly time series in the linear trend cases coincide with the ones in the nonlinear trend cases. The trend correctional method can effectively eliminate the influence of the long-term trends.

4. Validation with real-time indices

In this section, we examine the performance of the conventional and trend correctional methods using the realistic indices. In this case, a long-term trend series of a given series was computed with local regression using a weighted linear least square method and a first-degree polynomial model (with the span of a 30-yr period).

The first index that we examine is the global surface mean temperature index (GTI). As one can see, the GTI time series illustrates a clear global warming signal. The reference period of this trend is the climatological mean of 1951–1980. The trend appears nonlinear (Fig. 6a). The temporal correlation coefficient between the original time series and the nonlinear trend series is about 0.93.

As the GTI has a significant nonlinear trend, the anomaly time series derived based on the conventional method are affected by the trend (Fig. 6b). For instance, during the periods prior to the 1950s or post 1970s, the anomaly series are severely deviated from the true anomaly series. The bias depends on the intensity of the trend. For example, from the 1940s to 1960s, the trend is close to a constant. As a result, the bias is relatively small. During other periods, the trend is quite large, and so is the bias. In contrast, with the trend correctional method, the bias is markedly improved. The red line in Fig. 6c is very close to the true anomaly time series (black line).

It is worth mentioning that the standard deviation of the GTI is 0.37 while the standard deviation of the nonlinear trend series is 0.33. This implies that the nonlinear trend is an important part of the GTI. The nonparametric difference test (Kruskal–Wallis method) shows that there is no significant difference between the true anomaly time series (black line in Fig. 6c) and the trend correc-

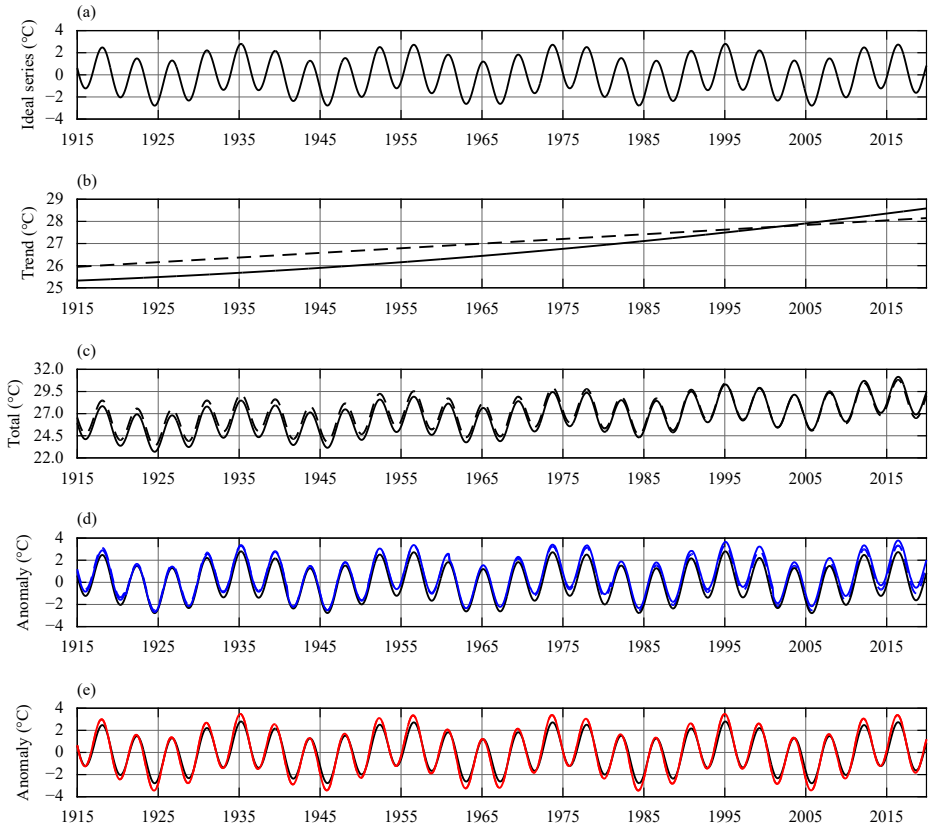

Fig. 4. As in Fig. 1, but for Cases 5 and 6. The black line in (d, e) denotes the true combined interannual and interdecadal signal specified.

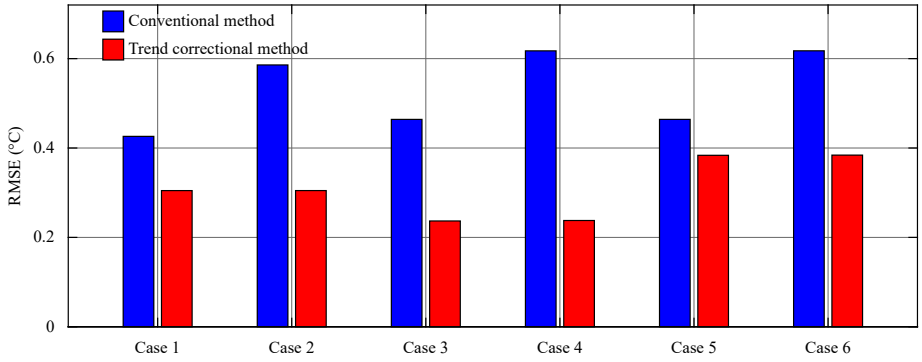

Fig. 5. The RMSEs for six cases. The red (blue) bars are the values calculated based on the trend correctional method (the conventional method).

tional method derived anomaly time series (red line in Fig. 6c). This is in great contrast with that derived based on the conventional method, which shows that such a nonlinear trend has a great non-local impact when a traditional method (i.e., the conventional method) is used.

In addition, we also examine other SST indices such as the IODE, IODW, TNA, and Niño 3.4 indices, shown in Fig. 7. Note that temporal CCs between time series derived by the trend correctional method and the observed detrended anomaly series are generally greater than those derived based on the conventional method, and RMSEs for the trend correctional method are less than those based on the conventional method. Take the Arctic SST index (ARC) as an example (Fig. 8). Although CC based on the trend correctional method is close to that based on the conventional method, there is a significant difference between the two anomaly time series (Figs. 8b, c). Its trend tends to be nonlinear (linear) after (before) the 1960s (Fig. 8a). As a consequence, it becomes obvious that the anomaly series calculated based on the conventional method shows a spurious rising trend after the 1990s (Fig. 8b), while the anomaly series calculated

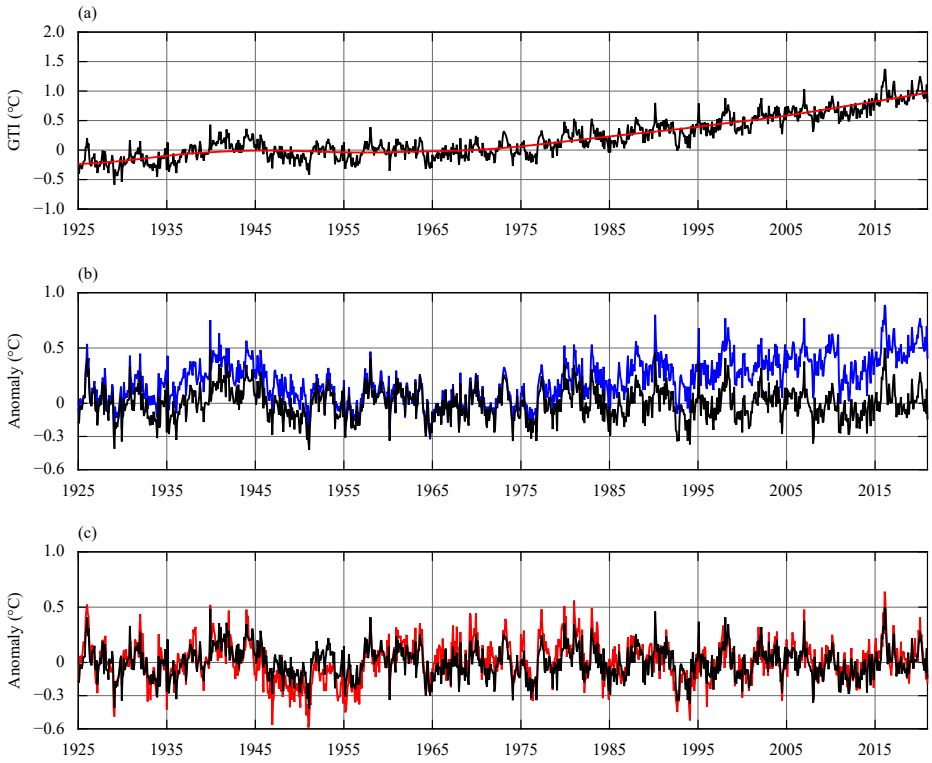

Fig. 6. The time series of (a) the original GTI (black line) and its long-term trend (red line), (b) the climate anomaly (blue line) computed with the conventional method and (c) the climate anomaly computed with the trend correctional method (red line). The black line in (b, c) denotes the observed climate anomaly with the long-term trend removed. The original GTI time series starts from 1880.

based on the trend correctional method coincides well with the observed anomaly signal (black line in Figs. 8b, c). Such a bias is well reflected in the RMSE chart (Fig. 7b).

Both the GTI and ARC discussed above show a clear

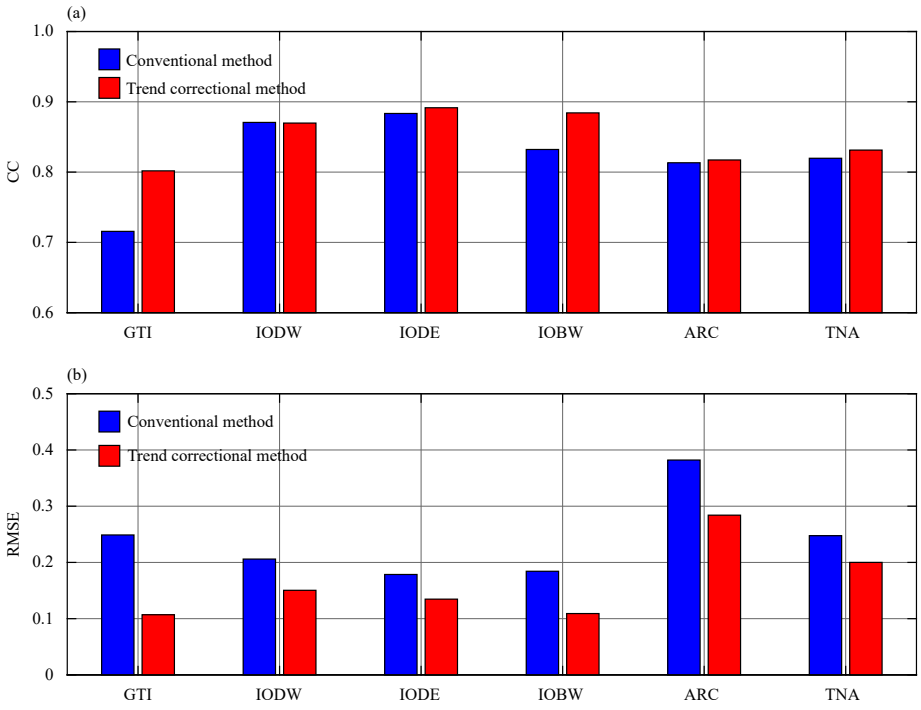

Fig. 7. CCs and RMSEs of the climate anomaly time series (with the long-term trend removed) derived based on the conventional method (blue) and trend correctional method (red) for real-time indices (GTI, IODW, IODE, IOBW, ARC, and TNA).

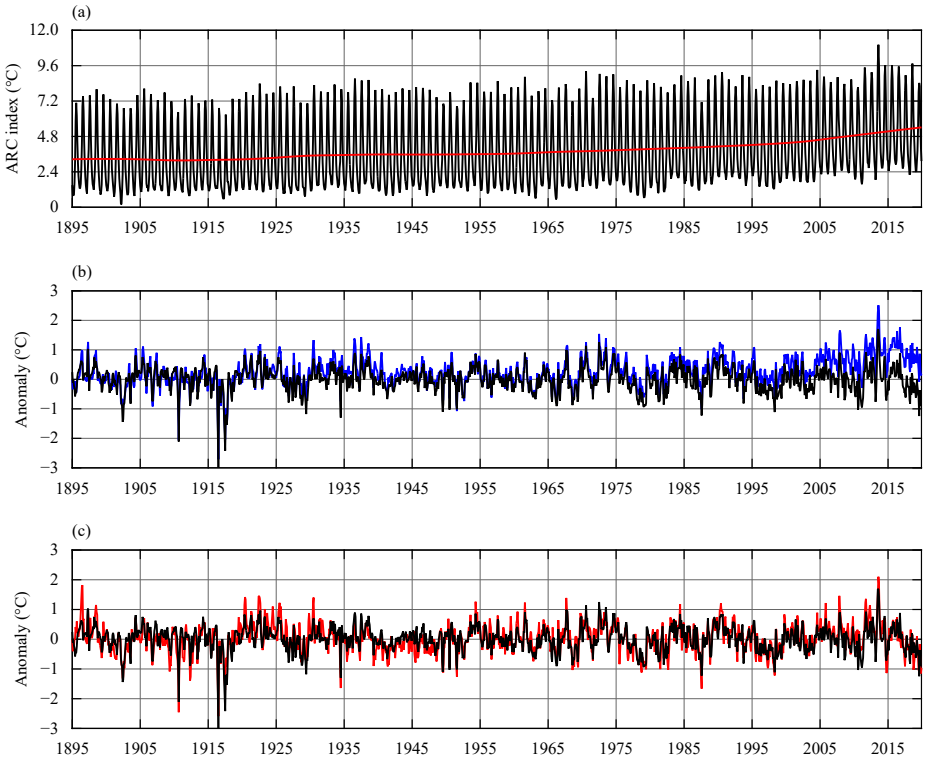

Fig. 8. As in Fig. 6, but for the ARC index. The ARC time series starts from 1850.

rising trend. As the Niño 3.4 index exhibits a weak long-term trend, would the two methods give rise to a similar result? Figure 9 illustrates the comparison of the two methods based on the Niño 3.4 index. Indeed, there is no significant difference between the two calculated anomaly time series by eye (Figs. 9b, c). However, there are some differences in power spectrum intensity and period, as shown in Fig. 10a. It is well known that the Niño 3.4 index contains two power spectrum peaks, one around 3–5 yr and another around 2 yr (e.g., Torrence and Compo, 1998; Li and Hsu, 2018). The anomaly time series derived based on the trend correctional method appears to have a stronger power in both the bands.

It shows that the variability of the global mean surface temperature is, to a certain extent, attributed to ENSO (e.g., Kosaka and Xie, 2013). To illustrate this, the correlation coefficients between GTI and Niño 3.4 index based on the two methods are computed. It turns out that CC for the conventional method time series is 0.19, whereas it is 0.44 for the trend correctional method calculated series. The latter is statistically significant.

A Mann–Kendall (MK) test is conducted for the Niño 3.4 anomaly series calculated by both the conventional and trend correctional methods. Due to the fact that the observed long-term trend is effectively removed, there is little trend in the trend correctional method time series (red curve in Fig. 10b). In the contrast, a significant long-term trend is found in the anomaly series derived based on the conventional method (blue curve in Fig. 10b). The bias is closely linked to the discontinuation of the 30-yr mean climatology defined by the conventional method, as the MK test of the climatology time series exhibits a significant trend (black curve in Fig. 10b).

5. Conclusions

A new method to calculate the climate anomalies is introduced in this paper. This method is named as trend correctional method. The formula to calculate the climate anomalies based on the original data is listed in Eq. (5) with proper coefficients listed in Table 1. The validation of this new method is demonstrated based on a comparison with the conventional method in which the climate anomalies are obtained by subtracting the original data from monthly climatology calculated based on the preceding three decades.

First, idealized interannual and interdecadal time series are examined. The reason to use the idealized time series is that we know the "true" signal so that it can be easily compared and validated. An idealized linear or nonlinear trend is superposed into the interannual or interdecadal signal to mimic an observed "raw" time series. Our calculations with the trend correctional and conventional methods demonstrate that the new method can effi-

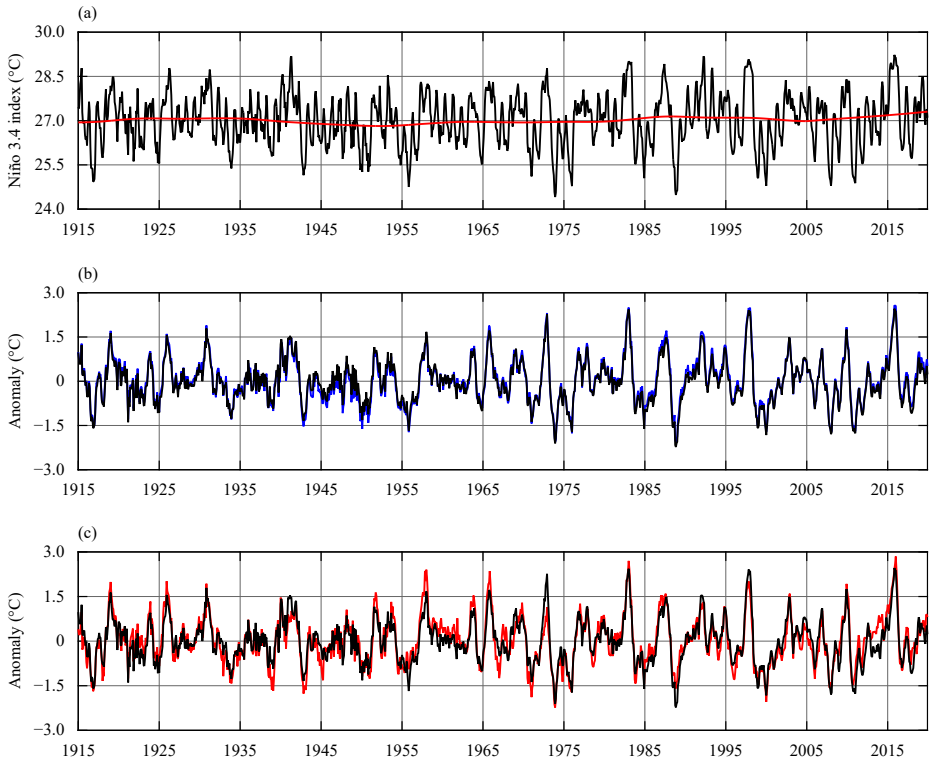

Fig. 9. As in Fig. 6, but for the Niño 3.4 index. The original Niño 3.4 index time series starts from 1870.

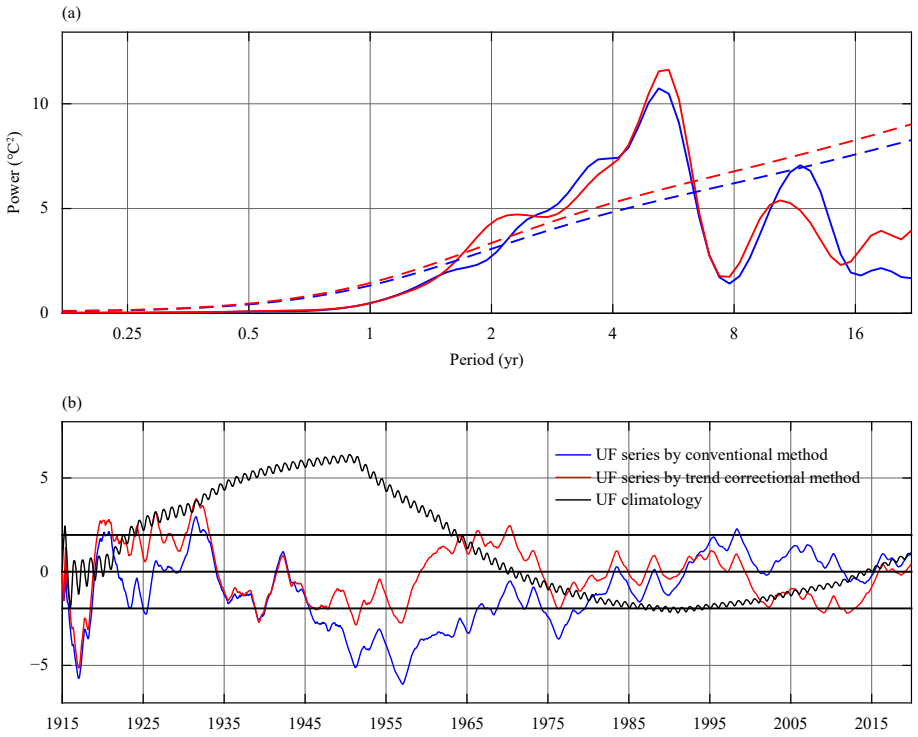

Fig. 10. (a) Power spectrum of the Niño 3.4 index derived from the conventional method (blue) and the trend correctional method (red). Dashed lines represent the 95% confidence level. (b) The MK test of the Niño 3.4 index derived from the conventional method (blue), the trend correctional method (red), and monthly climatology defined by the conventional method (black). A trend becomes statistically insignificant when the value is between two horizontal black lines.

ciently derive the "true" climate anomaly signal, especially in the nonlinear trend case. The generated time series resembles the "true" signal, with a much smaller RMSE in comparison to that derived from the conventional method. One characteristic of the anomaly series derived from the trend correctional method is a symmetry with respect to the value of 0, which makes it easy to identify cold (warm) events as the global mean temperature continues rising. Several spurious errors exist in the conventional method. There are artificial jump points in the first year of each decade and spurious rising trend within a 30-yr period. These problems become worse while there is an accelerated nonlinear trend. The aforementioned errors are largely eliminated when the trend correctional method is used.

Next, we examine the feasibility of the current method using the real-time indices. A few indices including the GTI, IOD, and Atlantic and Pacific Niño indices are examined. We demonstrate that the trend correctional method has a clear advantage in reproducing the observed anomaly time series. The anomaly time series derived based on the trend correctional method coincides well with the observed anomaly series while the time series derived based on the conventional method significantly deviates from the observed. As a result, both the temporal CC and RMSE are better with the trend correctional method. Even for a weak long-term trend case such as the Niño 3.4 index, the one derived based on the trend correctional method shows an advantage in the spectrum periods, correlation with the GTI and MK test.

Acknowledgments. The authors appreciate the use of the 20th Century Reanalysis Project version 2c dataset from the Office of Science Biological and Environmental Research (BER) at U.S. Department of Energy, the global surface mean temperature index from NASA, and the Niño indices from the NOAA Climate Program Office.

REFERENCES

Hansen, J., R. Ruedy, M. Sato, et al., 2010: Global surface temperature change. *Rev. Geophys.*, **48**, RG4004, doi: 10.1029/2010RG000345.

Hirahara, S., M. Ishii, and Y. Fukuda, 2014: Centennial-scale sea surface temperature analysis and its uncertainty. *J. Climate*, **27**, 57–75, doi: 10.1175/JCLI-D-12-00837.1.

Klein, S. A., B. J. Soden, and N.-C. Lau, 1999: Remote sea surface temperature variations during ENSO: Evidence for a tropical atmospheric bridge. *J. Climate*, **12**, 917–932, doi: 10.1175/1520-0442(1999)012<0917:RSSTVD>2.0.CO;2.

Kosaka, Y., and S.-P. Xie, 2013: Recent global-warming hiatus tied to equatorial Pacific surface cooling. *Nature*, **501**, 403–407, doi: 10.1038/nature12534.

Lau, K.-M., and H. Y. Weng, 1999: Interannual, decadal–interdecadal, and global warming signals in sea surface temperature during 1955–97. *J. Climate*, **12**, 1257–1267, doi: 10.1175/1520-0442(1999)012<1257:IDIAGW>2.0.CO;2.

Lau, N.-C., and M. J. Nath, 2000: Impact of ENSO on the variability of the Asian–Australian monsoons as simulated in GCM experiments. *J. Climate*, **13**, 4287–4309, doi: 10.1175/1520-0442(2000)013<4287:IOEOTV>2.0.CO;2.

Lenssen, N. J. L., G. A. Schmidt, J. E. Hansen, et al., 2019: Improvements in the GISTEMP uncertainty model. *J. Geophys. Res. Atmos.*, **124**, 6307–6326, doi: 10.1029/2018JD029522.

Li, T., and P.-C. Hsu, 2018: *Fundamentals of Tropical Climate Dynamics*. Springer, Cham, 229 pp. Available at https://link.springer.com/book/10.1007/978-3-319-59597-9. Accessed on 8 September 2021.

Meyers, G., 1996: Variation of indonesian throughflow and the El Niño–Southern Oscillation. *J. Geophys. Res. Oceans*, **101**, 12,255–12,263, doi: 10.1029/95JC03729.

Terray, P., and S. Dominiak, 2005: Indian Ocean sea surface temperature and El Niño–Southern Oscillation: A new perspective. *J. Climate*, **18**, 1351–1368, doi: 10.1175/JCLI3338.1.

Torrence, C., and G. P. Compo, 1998: A practical guide to wavelet analysis. *Bull. Amer. Meteor. Soc.*, **79**, 61–78, doi: 10.1175/1520-0477(1998)079<0061:APGTWA>2.0.CO;2.

Trenberth, K. E., 1997: The definition of El Niño. *Bull. Amer. Meteor. Soc.*, **78**, 2771–2777, doi: 10.1175/1520-0477(1997)078<2771:TDOENO>2.0.CO;2.

Trenberth, K. E., and D. P. Stepaniak, 2001: Indices of El Niño evolution. *J. Climate*, **14**, 1697–1701, doi: 10.1175/1520-0442(2001)014<1697:LIOENO>2.0.CO;2.

Turkington, T., B. Timbal, and R. Rahmat, 2019: The impact of global warming on sea surface temperature based El Niño–Southern Oscillation monitoring indices. *Int. J. Climatol.*, **39**, 1092–1103, doi: 10.1002/joc.5864.

Tech & Copy Editor: Zhirong CHEN